



Cite this: *Chem. Commun.*, 2019, 55, 794

Received 30th November 2018,
 Accepted 14th December 2018

DOI: 10.1039/c8cc09520e

rsc.li/chemcomm

Dramatic enhancement in pH sensitivity and signal intensity through ligand modification of a dicobalt PARACEST probe†

Agnes E. Thorarinsdottir  and T. David Harris *

The employment of an ancillary amine-substituted bisphosphonate ligand affords a dicobalt complex able to quantitate pH with a remarkably high sensitivity of 8.8(5) pH unit⁻¹ at 37 °C through a ratiometric paramagnetic chemical exchange saturation transfer (PARACEST) approach, where the different pH dependences of amine and amide CEST peak intensities are utilized.

Bioresponsive molecular magnetic resonance imaging (MRI) contrast agents are of tremendous interest for visualizing and monitoring biological processes.¹ MRI is ideally suited for molecular imaging *in vivo* owing to its high spatiotemporal image resolution and unlimited tissue penetration depth,² but bioresponsive contrast agents are needed to improve specificity and add valuable physiological information to the anatomical images.³ These molecular probes undergo changes in MRI signals in response to variations in biomarkers such as temperature,^{1a,c,4} pH,^{1a,c,5} redox status,^{1a,6} enzymes,^{1a,c,7} metal ions,^{1a,8} and metabolites,^{1a,c,9} and are therefore capable of reporting on their local physiological environment. In particular, pH-responsive probes are attractive since acidic extracellular pH is a prominent feature of various diseases and disorders.¹⁰ As such, the ability to differentiate small changes in pH through MRI is an important step toward improving the understanding, early detection, and treatment of pathologies.

In targeting pH-responsive MRI contrast agents, the employment of paramagnetic transition metal complexes that exploit the chemical exchange saturation transfer (CEST) mechanism is a promising strategy owing to their high sensitivity to environmental changes and tunability through ligand design.¹¹ Here, contrast is generated through proton exchange between the paramagnetic molecule and bulk H₂O upon frequency-specific irradiation.¹² The large chemical shifts of the exchangeable protons on these paramagnetic probes^{4b,5f,g,6c,d,13} improve sensitivity and specificity by minimizing overlap with biological background signals.¹⁴ Moreover, since the exchange rates of these ligand protons

typically show a strong pH dependence,^{5f,g,6c,13} a dramatic change in CEST signal intensity with pH can be achieved. However, due to the inherent concentration dependence of the intensity of CEST peaks, a ratiometric method is required to effectively exploit the CEST signal intensity for pH mapping in physiological environments, where the distribution of the probe is usually unknown. Toward this end, a single PARACEST probe that features two types of exchangeable protons that display markedly different pH-dependent changes in CEST signal intensity offers an ideal platform, as the ratio of the two peak intensities should be highly sensitive to pH variations.

We recently employed this approach to demonstrate the ability of dicobalt PARACEST probes to measure solution pH in a physiologically relevant range with high sensitivities of 0.99(7)–2.04(5) pH unit⁻¹.^{5f,g} These probes feature a phenoxo-centered tetra(carboxamide) ligand and an ancillary bisphosphonate ligand bearing amide and hydroxyl protons, respectively, with opposing pH-dependent CEST peak intensities (see Fig. 1, 1 and 2-X). Notably, the chemical shifts and intensities of the CEST signals could be tuned by chemically modifying the pendent amides and *para*-substituents on the phenoxo-centered ligand.^{5g} Building on these results, we sought to increase the pH sensitivity and signal intensities of this family of ratiometric PARACEST probes by modifying the ancillary bisphosphonate ligand. Herein, we report a new dicobalt complex that features an amine-substituted bisphosphonate ligand and exhibits dramatically enhanced pH sensitivity by virtue of an intense and pH-insensitive CEST signal from the distant amine group.

In an attempt to address the modest intensity and pH-dependent frequency of the etidronate hydroxyl CEST peak for our previously reported PARACEST probes,^{5f,g} we targeted the amine-substituted bisphosphonate ligand (L')⁴⁻, with the expectation that the equivalent amine protons would give rise to a stronger CEST effect. Furthermore, the different pK_a values of amine and amide protons have been shown to result in distinct pH-dependent changes in CEST peak intensity suitable for ratiometric pH sensing, albeit only for probes that exhibit small chemical shifts and modest pH sensitivity.¹⁵ As such, we envisioned that a dinucleating ligand

Department of Chemistry, Northwestern University, 2145 Sheridan Road, Evanston, IL, 60208-3113, USA. E-mail: dharris@northwestern.edu

† Electronic supplementary information (ESI) available: Experimental details and additional magnetic and spectroscopic data. See DOI: 10.1039/c8cc09520e

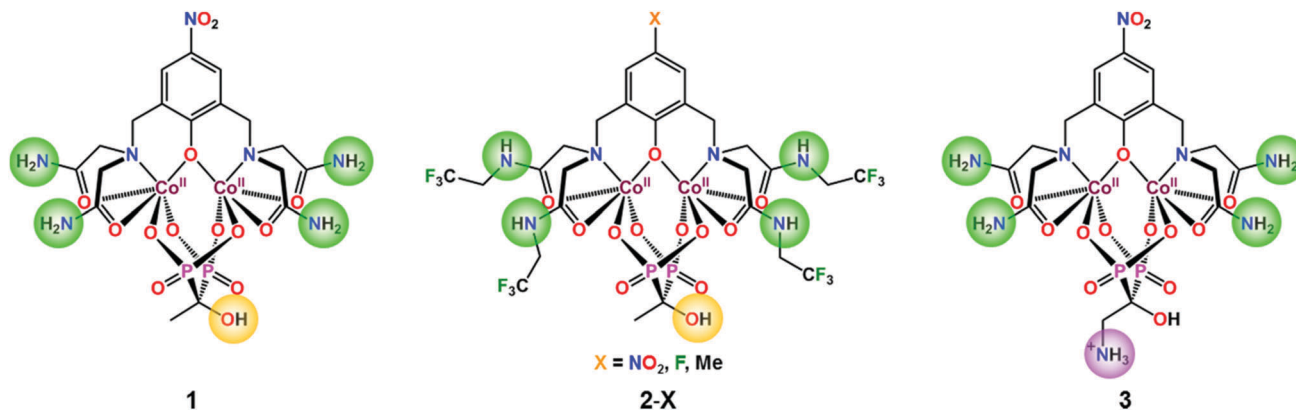


Fig. 1 Structures of previously reported dicobalt PARACEST pH probes $[\text{LCo}_2(\text{etidronate})]^-$ (left) and $[(\text{L}')\text{Co}_2(\text{etidronate})]^-$ (center), as observed in **1** and **2-X** ($X = \text{NO}_2, \text{F}, \text{Me}$), respectively, and the new dicobalt complex $\text{LCo}_2(\text{HL}')$ (right), as observed in **3**, reported here. The exchangeable amide, hydroxyl, and amine protons are highlighted in green, orange, and purple, respectively.

platform comprised of $(\text{L}')^{4-}$ and a phenoxo-centered tetra(carboxamide) ligand known for providing highly shifted and pH-sensitive amide CEST peaks could afford dicobalt PARACEST probes better suited for ratiometric pH quantitation.

Reaction of the nitro-substituted tetra(carboxamide) ligand HL with two equivalents of $\text{Co}(\text{NO}_3)_2 \cdot 6\text{H}_2\text{O}$ in the presence of one equivalent of $\text{H}_4\text{L}'$ in H_2O at pH 7.5 afforded $\text{Na}[\text{LCo}_2\text{L}'] \cdot 3.8\text{NaNO}_3 \cdot 5.9\text{H}_2\text{O}$ (see Fig. 1, **3**) as an orange solid (see Experimental section, ESI[†]). Slow diffusion of MeCN vapor into a concentrated H_2O solution of **3** gave light orange plate-shaped crystals that were not of sufficient quality for single-crystal X-ray diffraction analysis. However, the close similarity between the diffuse reflectance UV-visible spectra for **1'** and **3** (see Fig. S2, ESI[†]) suggests analogous solid-state structures.^{5f}

To assess the electronic structure of **3** in aqueous solution, UV-visible absorption spectra were collected for samples in 50 mM HEPES buffers with 100 mM NaCl. For a solution at pH 6.98, the spectrum exhibits a single strong peak at 371 nm ($\epsilon = 12\,400 \text{ M}^{-1} \text{ cm}^{-1}$) (see Fig. S3, ESI[†]), which is consistent with the spectra for **1** and **2-NO₂**^{5f,g} and can be unambiguously assigned to a ligand-metal charge transfer (LMCT) transition from the bridging phenolate to Co^{II} .¹⁶ Note that the position and intensity of this band are essentially identical between pH 6.1 and 8.0, indicating the presence of a single species in solution in this pH range. Based on precedent in amine-bisphosphonate molecular complexes,¹⁷ in conjunction with a notable increase in solubility of **3** at more alkaline pH, we assign this species to the neutral dicobalt complex $\text{LCo}_2(\text{HL}')$, where the amine of the bisphosphonate ligand is protonated.

The oxidation state and spin state of Co in **3** was further probed by variable-pH magnetic susceptibility measurements for aqueous buffer solutions at 37 °C using the Evans method.¹⁸ The $\chi_{\text{M}}T$ data do not significantly change in the pH range 6.1–8.0, affording an average value of $\chi_{\text{M}}T = 5.96(6) \text{ cm}^3 \text{ K mol}^{-1}$ (see Fig. S4 and Table S1, ESI[†]). These data are in good agreement with those obtained for **1** and **2-X**, indicative of pseudo-octahedral high-spin Co^{II} centers ($S = 3/2$) with significant magnetic anisotropy.^{5f,g,11a,16b,19}

To further probe the solution structure and properties of **3**, ¹H NMR spectra were collected at 37 °C for aqueous solutions

buffered to selected pH values. The spectrum at pH 7.02 exhibits sharp and paramagnetically shifted resonances with chemical shifts from –103 to 182 ppm versus H_2O (see Fig. S5, upper, ESI[†]), consistent with the presence of high-spin Co^{II} .¹¹ Comparison to the spectrum recorded in D_2O (see Fig. S5, lower, ESI[†]) and the spectrum for **1** at pH 7.06 (see Fig. S6, ESI[†]) reveals that the resonances at 4, 6, 11, 13, 66, 68, 103, and 106 ppm correspond to four sets of two slightly inequivalent amide protons, whereas the peaks at 48 and 101 ppm correspond to amine and hydroxyl protons on $(\text{HL}')^{3-}$, respectively. Furthermore, the two methylene protons on $(\text{HL}')^{3-}$ resonate at 69 and 74 ppm, in accord with the etidronate methyl peak at 66 ppm for **1**. Together, these observations indicate pseudo- C_2 symmetry of $\text{LCo}_2(\text{HL}')$ in **3**, as observed for the anionic complexes in **1** and **2-X**.^{5f,g} Moreover, the close similarity between the ¹H NMR profiles for **1** and **3** corroborates our previous observations that the chemical shifts of resonances from L^- are not significantly affected by modest modifications of the bisphosphonate ligand.^{5f} Importantly, the amine resonance for **3** is highly shifted and well separated from the amide peaks, suggesting the potential utility of these two functional groups for pH sensing using ratiometric PARACEST. Finally, whereas no chemical shift changes are observed upon increasing the pH from 5.99 to 7.80, the exchangeable proton resonances broaden significantly, indicating faster proton exchange (see Fig. S7, ESI[†]).

To further investigate the possibility of employing **3** as a pH-responsive PARACEST probe, variable-pH CEST spectra were collected at 37 °C for 9 mM solutions of **3** in HEPES buffers. The spectrum at pH 6.01 exhibits three peaks at 48, 67, and 100 ppm with 36, 2.1, and 4.8% CEST intensity, respectively (see Fig. 2, upper). The CEST peaks at 48 and 67 ppm correspond to amine and two overlapping amide resonances, respectively, as evidenced by ¹H NMR analysis. As the pH is raised to 7.58, the intensity of the amine peak remains relatively constant, reaching a maximum value of 42% at pH 7.01. However, further increasing the pH to 7.78 leads to a significant peak broadening and concurrent intensity reduction (see Fig. 2). In stark contrast, the CEST effect at 67 ppm increases nearly linearly in this pH range, affording a maximum value of 23% at pH 7.78 (see Fig. 2). This increase in CEST peak intensity with pH is consistent with the base-catalyzed amide proton exchange

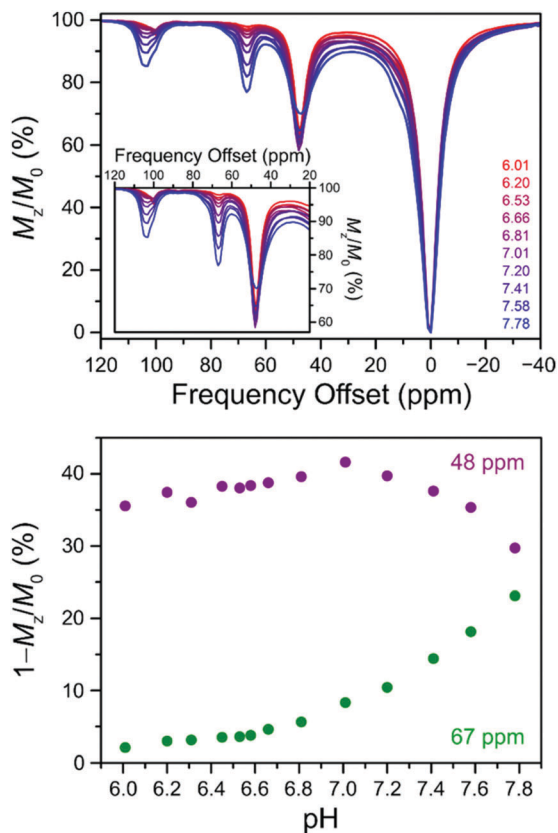


Fig. 2 Upper: Variable-pH CEST spectra collected at 11.7 T and 37 °C using a 2 s presaturation pulse and $B_1 = 22 \mu\text{T}$ for 9 mM aqueous solutions of **3** with 50 mM HEPES and 100 mM NaCl buffered to pH 6.01–7.78 (see legend). Inset: Expanded view of the CEST peaks of interest. Lower: Plot of CEST intensities from presaturation at 48 ppm (purple) and 67 ppm (green) versus pH.

observed for **1** and **2-X**.^{5f,g} Indeed, exchange rate analysis using the Omega plot method²⁰ reveals that the rate constant (k_{ex}) for the amide protons at 67 ppm for **3** increases from $2.9(4) \times 10^2$ to $6.1(1) \times 10^2 \text{ s}^{-1}$ between pH 6.53 and 7.78 (see Fig. S8 and S10, ESI[†]). These values agree well with those previously reported for dicobalt complexes of L^- .^{5f} To compare, k_{ex} for the amine protons in **3** exhibits a relatively small pH dependence below pH 7.0 but then undergoes a dramatic increase when the pH is raised further, reaching a maximum of $k_{\text{ex}} = 1.5(1) \times 10^3 \text{ s}^{-1}$ at pH 7.78 (see Fig. S9 and S10, ESI[†]). These observations are consistent with NMR line width and CEST intensity analyses, indicating that $k_{\text{ex}} = 800\text{--}900 \text{ s}^{-1}$ provides optimal amine CEST effect for the dinuclear system. Finally, note that the CEST peak at 100–103 ppm stems from overlapping amide and hydroxyl resonances, as observed for **1**.^{5f} Despite the high chemical shift, the broadness of this peak and pH-dependent frequency render it unsuitable for use in ratiometric pH quantitation.

The markedly different pH dependences of the amine and amide CEST intensities at 48 and 67 ppm, respectively, prompted us to assess the utility of **3** in the ratiometric quantitation of pH. Indeed, the ratio of CEST intensities at 48 and 67 ppm ($\text{CEST}_{48\text{ppm}}/\text{CEST}_{67\text{ppm}}$) exhibits a pronounced pH dependence. Upon increasing the pH from 6.20 to 7.41, $\text{CEST}_{48\text{ppm}}/\text{CEST}_{67\text{ppm}}$ shows a linear

decrease and a fit to the data provided a pH calibration curve with the following equation (see Fig. 3):

$$\text{CEST}_{48\text{ppm}}/\text{CEST}_{67\text{ppm}} = -8.8 \times \text{pH} + 67 \quad (1)$$

Remarkably, the pH sensitivity of 8.8(5) for **3**, as estimated by the absolute value of the slope of the linear calibration curve, is over 4-fold higher than for other dicobalt complexes in this family of PARACEST pH probes.^{5f,g} In fact, to our knowledge, **3** exhibits the highest pH sensitivity in the physiological range yet reported for a ratiometric MR-based paramagnetic probe at 37 °C.²¹ The dramatic increase in pH sensitivity for **3** stems from the linear relationship between $\text{CEST}_{48\text{ppm}}/\text{CEST}_{67\text{ppm}}$ and pH, rather than the logarithm of the intensity ratios, as observed for all previously reported dicobalt analogues.^{5f,g} Importantly, the pH calibration curve for **3** is not significantly affected by the concentration of the complex, as the slopes obtained for 5 and 9 mM samples of **3** fall within error of one another (see Fig. S11–S16, ESI[†]). This observation illustrates that the ratiometric method using **3** provides a concentration-independent measure of pH in the range 6.20–7.41, which is in line with previous findings for **1** and **2-X**.^{5f,g} Taken together, these results show that a substantial sensitivity improvement in ratiometric pH quantitation is achieved by using an amine-functionalized dinucleating ligand platform. Furthermore, the amine group from $(\text{HL}')^{3-}$ affords a CEST peak with much higher intensity than does the etidronate hydroxyl group in **1** and **2-X**.^{5f,g}

The observation of no shifts in ^1H NMR frequencies between pH 6.0 and 7.8 for **3** contrasts with that of **1** and **2-X**,^{5f,g} suggesting that the pK_{a} corresponding to protonation of one of the cobalt-coordinated O_{L} atoms (see Fig. S17, ESI[†]) is significantly lower for **3** than for **1** and **2-X**.^{5f,g} Indeed, sigmoidal fits (see Experimental section, ESI[†]) to the chemical shift versus pH data for the two methylene resonances from the bisphosphonate ligand between pH 1.50 and 7.80 gave values of $\text{pK}_{\text{a}} = 3.57(8)$ and $3.96(4)$ for **3** (see Fig. S18, ESI[†]). The slight discrepancy between the pK_{a} values estimated from the two protons likely arises from their different distances from the O_{L} atoms. Most importantly, both values are substantially lower than those of 5.01(3) and 4.76(7) reported for **1** and **2-NO₂**, respectively,^{5f,g} indicating that pH-induced shifts in

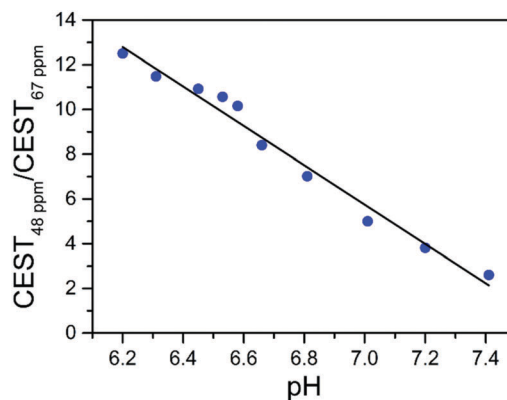


Fig. 3 Plot of the ratios of CEST intensities from presaturation at 48 and 67 ppm for 9 mM aqueous buffer solutions of **3** versus pH. Circles denote experimental data and the line corresponds to a linear fit to the data.

CEST peak frequencies in the physiological pH range can be prevented for this family of probes by decreasing the pK_a of the ionization process below 4.0. This is highly advantageous for intensity-based PARACEST probes and was accomplished for 3 through incorporation of a protonated amine group.

Finally, the high solution stability of 3 was confirmed by cyclic voltammetry and ligand substitution studies. The absence of an oxidation process within the potential window of the solvent indicates that 3 is inert toward reaction with O_2 in aqueous solutions (see Fig. S19, ESI[†]).²² Moreover, 3 remains intact in the presence of physiological phosphates, demonstrating its high kinetic inertness (see Fig. S20, ESI[†]).

The foregoing results demonstrate the utility of a new amine-functionalized dicobalt PARACEST probe for the ratiometric quantitation of pH, and highlight the excellent tunability of the dinucleating ligand platform to enhance pH sensitivity and CEST signal intensities. Efforts are underway to investigate the stability and performance of this probe in physiological environments. Toward this end, preliminary NMR and CEST experiments for 3 in fetal bovine serum (FBS) and 17% (w/v) gelatin gels revealed similar pH-dependent trends and linear pH calibration curves as observed in HEPES buffers. Note, however, that the pH calibration equation is slightly affected by the surrounding medium owing to differences in proton exchange rates and/or T_1 relaxation times between media (see Fig. S21–S33 and Tables S2–S4, ESI[†]). Thus, for *in vivo* studies, the pH calibration curve must be constructed in a medium that closely mimics the targeted environment.

This research was funded by Northwestern University. A. E. T. acknowledges the Leifur Eiriksson Foundation for funding support. We thank Prof. T. J. Meade for use of his HPLC system and lyophilizer, and Dr. D. Z. Zee for helpful discussions.

Conflicts of interest

There are no conflicts to declare.

Notes and references

- (a) D. V. Hingorani, A. S. Bernstein and M. D. Pagel, *Contrast Media Mol. Imaging*, 2015, **10**, 245–265; (b) G. Angelovski, *Angew. Chem., Int. Ed.*, 2016, **55**, 7038–7046; (c) S. Sinharay and M. D. Pagel, *Annu. Rev. Anal. Chem.*, 2016, **9**, 95–115.
- (a) P. Caravan, J. J. Ellison, T. J. McMurry and R. B. Lauffer, *Chem. Rev.*, 1999, **99**, 2293–2352; (b) V. Rieke and K. B. Pauly, *J. Magn. Reson. Imaging*, 2008, **27**, 376–390.
- R. Weissleder, B. D. Ross, A. Rehemtulla and S. S. Gambhir, *Molecular Imaging: Principles and Practice*, People's Medical Publishing House, Shelton, CT, 2010.
- (a) S. Zhang, C. R. Malloy and A. D. Sherry, *J. Am. Chem. Soc.*, 2005, **127**, 17572–17573; (b) I.-R. Jeon, J. G. Park, C. R. Haney and T. D. Harris, *Chem. Sci.*, 2014, **5**, 2461–2465; (c) P. B. Tsitovich, J. M. Cox, J. B. Benedict and J. R. Morrow, *Inorg. Chem.*, 2016, **55**, 700–716; (d) A. E. Thorarinsdottir, A. I. Gaudette and T. D. Harris, *Chem. Sci.*, 2017, **8**, 2448–2456.
- (a) S. Aime, D. D. Castelli and E. Terreno, *Angew. Chem., Int. Ed.*, 2002, **41**, 4334–4336; (b) Y. Wu, T. C. Soesbe, G. E. Kiefer, P. Zhao and A. D. Sherry, *J. Am. Chem. Soc.*, 2010, **132**, 14002–14003; (c) Y. Huang, D. Coman, P. Herman, J. U. Rao, S. Maritim and F. Hyder, *NMR Biomed.*, 2016, **29**, 1364–1372; (d) K.-L. N. A. Finney, A. C. Harnden, N. J. Rogers, P. K. Senanayake, A. M. Blamire, D. O'Hogain and D. Parker, *Chem. – Eur. J.*, 2017, **23**, 7976–7989; (e) A. I. Gaudette, A. E. Thorarinsdottir and T. D. Harris, *Chem. Commun.*, 2017, **53**, 12962–12965; (f) A. E. Thorarinsdottir, K. Du, J. H. P. Collins and T. D. Harris, *J. Am. Chem. Soc.*, 2017, **139**, 15836–15847; (g) A. E. Thorarinsdottir, S. M. Tatro and T. D. Harris, *Inorg. Chem.*, 2018, **57**, 11252–11263.
- (a) S. J. Ratnakar, S. Viswanathan, Z. Kovacs, A. K. Jindal, K. N. Green and A. D. Sherry, *J. Am. Chem. Soc.*, 2012, **134**, 5798–5800; (b) G. S. Loving, S. Mukherjee and P. Caravan, *J. Am. Chem. Soc.*, 2013, **135**, 4620–4623; (c) P. B. Tsitovich, J. A. Sperry and J. R. Morrow, *Angew. Chem., Int. Ed.*, 2013, **52**, 13997–14000; (d) K. Du, E. A. Waters and T. D. Harris, *Chem. Sci.*, 2017, **8**, 4424–4430.
- (a) R. A. Moats, S. E. Fraser and T. J. Meade, *Angew. Chem., Int. Ed.*, 1997, **36**, 726–728; (b) S. Mizukami, R. Takikawa, F. Sugihara, Y. Hori, H. Tochio, M. Wälchli, M. Shirakawa and K. Kikuchi, *J. Am. Chem. Soc.*, 2008, **130**, 794–795; (c) T. Chauvin, P. Durand, M. Bernier, H. Meudal, B.-T. Doan, F. Noury, B. Badet, J.-C. Beloil and E. Tóth, *Angew. Chem., Int. Ed.*, 2008, **47**, 4370–4372.
- (a) E. L. Que and C. J. Chang, *J. Am. Chem. Soc.*, 2006, **128**, 15942–15943; (b) J. L. Major, G. Parigi, C. Luchinat and T. J. Meade, *Proc. Natl. Acad. Sci. U. S. A.*, 2007, **104**, 13881–13886; (c) A. Bar-Shir, A. A. Gilad, K. W. Y. Chan, G. Liu, P. C. M. van Zijl, J. W. M. Bulte and M. T. McMahon, *J. Am. Chem. Soc.*, 2013, **135**, 12164–12167.
- (a) S. Aime, D. D. Castelli, F. Fedeli and E. Terreno, *J. Am. Chem. Soc.*, 2002, **124**, 9364–9365; (b) M. G. Shapiro, G. G. Westmeyer, P. A. Romero, J. O. Szablowski, B. Küster, A. Shah, C. R. Otey, R. Langer, F. H. Arnold and A. Jasanoff, *Nat. Biotechnol.*, 2010, **28**, 264–270.
- (a) I. F. Tannock and D. Rotin, *Cancer Res.*, 1989, **49**, 4373–4384; (b) Y. Kato, S. Ozawa, C. Miyamoto, Y. Maehata, A. Suzuki, T. Maeda and Y. Baba, *Cancer Cell Int.*, 2013, **13**, 89–96; (c) K. Rajamäki, T. Nordström, K. Nurmi, K. E. O. Åkerman, P. T. Kovanen, K. Öörni and K. K. Eklund, *J. Biol. Chem.*, 2013, **288**, 13410–13419.
- (a) T. L. James, *Nuclear Magnetic Resonance in Biochemistry: Principles and Applications*, Academic Press, New York, NY, 1975; (b) I. Bertini and C. Luchinat, *NMR of Paramagnetic Molecules in Biological Systems*, The Benjamin/Cummings Publishing Company Inc., Menlo Park, CA, 1986.
- K. M. Ward, A. H. Aletras and R. S. Balaban, *J. Magn. Reson.*, 2000, **143**, 79–87.
- (a) S. J. Dorazio, P. B. Tsitovich, K. E. Sifers, J. A. Sperry and J. R. Morrow, *J. Am. Chem. Soc.*, 2011, **133**, 14154–14156; (b) S. J. Dorazio, A. O. Olatunde, J. A. Sperry and J. R. Morrow, *Chem. Commun.*, 2013, **49**, 10025–10027.
- (a) S. D. Wolff and R. S. Balaban, *Magn. Reson. Med.*, 1989, **10**, 135–144; (b) M. Zaiss and P. Bachert, *Phys. Med. Biol.*, 2013, **58**, R221–R269.
- (a) G. Liu, Y. Li and M. D. Pagel, *Magn. Reson. Med.*, 2007, **58**, 1249–1256; (b) G. Liu, Y. Li, V. R. Sheth and M. D. Pagel, *Mol. Imaging*, 2012, **11**, 47–57; (c) V. R. Sheth, G. Liu, Y. Li and M. D. Pagel, *Contrast Media Mol. Imaging*, 2012, **7**, 26–34; (d) V. R. Sheth, Y. Li, L. Q. Chen, C. M. Howison, C. A. Flask and M. D. Pagel, *Magn. Reson. Med.*, 2012, **67**, 760–768.
- (a) F. B. Johansson, A. D. Bond, U. G. Nielsen, B. Moubaraki, K. S. Murray, K. J. Berry, J. A. Larrabee and C. J. McKenzie, *Inorg. Chem.*, 2008, **47**, 5079–5092; (b) J.-L. Tian, W. Gu, S.-P. Yan, D.-Z. Liao and S.-H. Jiang, *Z. Anorg. Allg. Chem.*, 2008, **634**, 1775–1779.
- (a) N. Margiotta, R. Ostuni, V. Gandin, C. Marzano, S. Piccinonna and G. Natile, *Dalton Trans.*, 2009, 10904–10913; (b) B. Demoro, F. Caruso, M. Rossi, D. Benítez, M. González, H. Cerecetto, M. Galizzi, L. Malayil, R. Docampo, R. Faccio, A. W. Momburú, D. Gambino and L. Otero, *Dalton Trans.*, 2012, **41**, 6468–6476.
- (a) D. F. Evans, *J. Chem. Soc.*, 1959, 2003–2005; (b) E. M. Schubert, *J. Chem. Educ.*, 1992, **69**, 62.
- (a) H. Sakiyama, R. Ito, H. Kumagai, K. Inoue, M. Sakamoto, Y. Nishida and M. Yamasaki, *Eur. J. Inorg. Chem.*, 2001, 2027–2032; (b) M. J. Hossain, M. Yamasaki, M. Mikuriya, A. Kuribayashi and H. Sakiyama, *Inorg. Chem.*, 2002, **41**, 4058–4062.
- W. T. Dixon, J. Ren, A. J. M. Lubag, J. Ratnakar, E. Vinogradov, I. Hancu, R. E. Lenkinski and A. D. Sherry, *Magn. Reson. Med.*, 2010, **63**, 625–632.
- D. L. Longo, P. Z. Sun, L. Consolino, F. C. Michelotti, F. Uggeri and S. Aime, *J. Am. Chem. Soc.*, 2014, **136**, 14333–14336.
- P. M. Wood, *Biochem. J.*, 1988, **253**, 287–289.